World Journal of Engineering Research
ISSN: 2959-9873
DOI: https://doi.org/10.61784/wjer3027

DIAGNOSIS FOR WHEELSET OUT-OF-ROUNDNESS OF METRO VEHICLE USING VMD COMBINED WITH OPTIMIZED MCKD

XiChun Luo, HaoRan Hu*
Yunnan Jingjian Rail Transit Investment Construction Co., Ltd., Kunming 650000, Yunnan, China.
Corresponding Author: HaoRan Hu, Email: 1225372272@qq.com

Abstract: Wheel out-of-roundness (OOR) is a prevalent issue in rail transit vehicles, posing potential safety hazards to electric multiple units (EMUs) and significantly affecting passenger ride comfort. However, current research predominantly focuses on dynamic simulation analyses, with relatively few studies targeting the vibration characteristics associated with wheel OOR. To address this gap, this paper proposes a novel diagnostic method that utilizes Variational Mode Decomposition (VMD) to extract salient signal features and employs the Grey Wolf Optimizer (GWO) to determine the optimal parameters for Maximum Correlated Kurtosis Deconvolution (MCKD) based on minimum sample entropy. Finally, the fault characteristic frequencies are extracted through envelope spectrum analysis. The method was validated on real-world wheel OOR data collected from operational trains. The results demonstrate that the proposed approach effectively isolates the fault characteristic information of wheel OOR, providing a robust basis for further research and practical application in this domain.
Keywords: Wheel out-of-roundness; Variational Mode Decomposition; Maximum Correlated Kurtosis Deconvolution; Greywolf optimizer

1 INTRODUCTION

Wheel out-of-roundness (OOR) faults are primarily manifested as polygonal wheels, characterized by a periodic radial deviation along the wheel circumference, resulting in irregular rolling profiles. Currently, wheel OOR detection methods are mainly categorized into two types: quantitative measurements using wheel dimension gauges and dynamic qualitative detection utilizing imaging or laser-based techniques. Typical wheel dimension tools include wheel diameter gauges, the so-called “Type IV gauge”, and lathe-based measurement systems. These approaches are generally static, require cumbersome procedures, and cannot provide continuous monitoring of polygonal wear development. In contrast, dynamic detection techniques based on imaging and similar technologies enable continuous tracking of wheel OOR and localization of the fault; however, they lack the ability to precisely quantify polygonal wear patterns[1]. Hou et al. summarized the state-of-the-art developments in wheel tread scratch detection systems and highlighted key technical challenges in field implementation[2]. Ji investigated automatic measurement technologies for wheel geometric dimensions, providing a basis for online dynamic monitoring[3].

When a wheel OOR fault occurs, the periodic contact between the irregular wheel tread and the rail generates cyclic impact signals. Therefore, an essential challenge in wheel OOR fault diagnosis is how to effectively extract these impact signals and accurately identify the characteristic fault frequencies during operation. To address this, Zhang et al. proposed a method combining autocorrelation-based denoising and Variational Mode Decomposition (VMD)[4], demonstrating the superiority of VMD in extracting periodic fault features. Sun et al. introduced a VMD and Singular Value Decomposition (SVD) hybrid denoising technique and verified[5], through comparison with traditional wavelet and Empirical Mode Decomposition (EMD) methods, its enhanced capability in suppressing complex noise. Fei validated that the Maximum Correlated Kurtosis Deconvolution (MCKD) algorithm exhibits robust noise resistance and strong capability to extract impulsive features[6], allowing precise identification of weak fault frequencies. Zhao further demonstrated that optimizing classifier network parameters using the Grey Wolf Optimizer (GWO) significantly improves recognition accuracy[7].

Motivated by these advancements, this study proposes an integrated approach combining VMD and GWO-optimized MCKD for wheel OOR fault diagnosis. First, the acquired vibration signals are decomposed by VMD to obtain multiple Intrinsic Mode Functions (IMFs). Key IMFs are then selected and reconstructed based on the cross-correlation coefficient criterion. To enhance the recognition accuracy of MCKD, sample entropy is introduced as an evaluation metric, and the GWO is employed to optimize MCKD parameters for locating the impulsive components, thereby enabling reliable extraction of fault characteristics[8].

2 METHODS

2.1 VMD

VMD is an adaptive signal processing technique that determines the optimal solution for each decomposed mode’s center frequency through iterative search, enabling automatic decomposition of a signal into modal components with compact frequency bandwidths [9].

The VMD method decomposes a signal by introducing it into a variational framework to obtain Intrinsic Mode

Functions (IMFs). The bandwidth and center frequency of each IMF are updated iteratively and alternately in a self-adaptive manner until convergence is achieved. This results in the signal being decomposed into a predefined number, *K*, of IMFs. For a given signal *f*, the objective is to search for *K* mode functions u_k (k) such that the sum of their estimated bandwidths is minimized [10]. The decomposition procedure for each mode consists of the following steps:

(1) For each mode function u_k (k), a Hilbert transform is performed to obtain its analytic signal:

$$\left[\delta(t)+\frac{j}{\pi t}\right]*u_k(t) \tag{1}$$

Where t denotes time; $\delta(t)$ is the Dirac delta function; and $\{u_k\}=\{u_1,\cdots,u_k\}$ are the IMF components extracted by decomposition. Multiplication by $e^{-j\omega_k t}$ shifts each mode's spectrum to baseband, aligning its center frequency to zero for bandwidth estimation:

$$\left[\delta(t)+\frac{j}{\pi t}\right]*u_k(t)e^{-j\omega_k t} \tag{2}$$

Where $\{\omega_k\}==\{\omega_1,\cdots,\omega_k\}$ denotes the center frequencies of the corresponding IMF components $u_k(t)$.

(2) The bandwidth of each mode is estimated by calculating the squared H^1 norm (smoothness) of the demodulated signal. Thus, the constrained variational model can be formulated as:

$$\begin{aligned}&\min_{\{u_k\},\{\omega_k\}}\left\{\sum_k\left\|\delta_t\left[\left(\delta(t)+\frac{j}{\pi t}\right)*u_k(t)\right]e^{-j\omega_k t}\right\|_2^2\right\}\\&s.t.\sum_k u_k=f\end{aligned} \tag{3}$$

To transform the constrained variational problem into an unconstrained one, a quadratic penalty factor α and a Lagrangian multiplier $\lambda(t)$ are introduced. Here, $\lambda(t)$ ensures strict satisfaction of the reconstruction constraint, while α maintains high reconstruction accuracy for noisy signals. The augmented Lagrangian expression is given by:

$$\begin{aligned}&\left(\{u_k\},\{\omega_k\},\lambda\right)=\alpha\sum_k\left\|\partial_t\left[\left(\partial(t)+\frac{j}{\pi t}\right)*u_k(t)\right]e^{-j\omega_k t}\right\|_2^2\\&+\left\|f(t)-\sum_k u_k(t)\right\|_2^2+\left\langle\lambda(t),f(t)-\sum_k u_k(t)\right\rangle\end{aligned} \tag{4}$$

Using the Alternating Direction Method of Multipliers (ADMM), u_k^{n+1}, ω_k^{n+1}, and λ^{n+1} are iteratively updated to find the saddle point of the augmented Lagrangian with respect to each u_k:

$$u_k^{n+1}=\arg\min_{u_k\in X}\left\{\alpha\left\|\partial_t\left[\left(\delta(t)+\frac{j}{\pi t}\right)*u_k(t)\right]e^{-j\omega_k t}\right\|_2^2+\left\|f(t)-\sum_i u_i(t)+\frac{\lambda(t)}{2}\right\|_2^2\right\} \tag{5}$$

Here, ω_k corresponds to ω_k^{n+1}, and $\sum u_i(t)$ corresponds to $\sum_{i\neq k}u_i(t)^{n+1}$. By applying the Fourier transform and substituting $\omega-\omega_k$ for ω, the constrained variational problem is converted into an unconstrained quadratic optimization form as follows:

$$\hat{u}_k^{\,n+1}(\omega)=\frac{\hat{f}(\omega)-\sum_{i\neq k}\hat{u}_i(\omega)+\frac{\hat{\lambda}(\omega)}{2}}{1+2\alpha(\omega-\omega_k)^2} \tag{6}$$

Based on this procedure, the center frequency is updated according to:

$$\omega_k^{n+1}=\frac{\int_0^\infty\omega\left|\hat{u}_k(\omega)\right|^2d\omega}{\int_0^\infty\left|\hat{u}_k(\omega)\right|^2d\omega} \tag{7}$$

Here, $\hat{u}_k(\omega)$ denotes the current residual component's Wiener-filtered estimate, calculated as $\hat{f}(\omega)-\sum_{i\neq k}\hat{u}_i(\omega)$. The updated ω_k^{n+1} is the centroid of the current mode's power spectrum. Applying the inverse Fourier transform to $\{\hat{u}_k(\omega)\}$ yields the time-domain mode functions $\{\hat{u}_k(t)\}$. The iterative algorithm proceeds as follows:

① Initialize $\{u_k^1\}$, $\{\omega_k^1\}$, λ^1, and set n = 0;

② Let n=n+1 and repeat the full cycle;

③ Update u_k and ω_k;

④ Increment k=k+1, repeat step ③ until k=K;

⑤ Update the Lagrange multiplier λ according to $\lambda^{n+1}=\lambda^n+\tau\left(f-\sum u_k^{n+1}\right)$;

⑥ Check the convergence criterion ξ>0; repeat the iteration until the stopping condition is satisfied:

$$\sum_{k=1}^{K}\frac{\left\|\hat{u}_k^{n+1}(\omega)-\hat{u}_k^n(\omega)\right\|}{\left\|\hat{u}_k^n(\omega)\right\|_2^2}<\varepsilon.$$

2.2 MCKD

To enhance the traditional Minimum Entropy Deconvolution (MED) technique by incorporating fault periodicity, a new evaluation criterion—correlated kurtosis—is introduced. Correlated kurtosis, denoted as $CK_M(T)$, addresses the insensitivity of standard kurtosis to periodic impacts and allows reliable detection of periodic impulsive signals [11]. The correlated kurtosis of the zero-mean signal y_n is defined as:

$$CK_M(T)=\frac{\sum_{n=1}^{N}(\prod_{m=0}^{M}y_{n-mT})^2}{(\sum_{n=1}^{N}y_n^{\,2})^{M+1}} \tag{8}$$

Where, $y=\sum_{k=1}^{L}f_k x_{n-k+1}$;

N is the data length;

T is the period of the fault-induced impulsive signal;

M is the number of shift periods;

L is the length of the FIR filter;

y_{n-mT} denotes the vibration signal at time $n-mT$.

The principle of MCKD is to find a specific filter—namely, a finite impulse response (FIR) filter $f(n)$ —that maximizes the correlated kurtosis of $x(n)$, thereby extracting impulsive features for fault diagnosis [12]. Compared with the traditional Minimum Entropy Deconvolution (MED), the MCKD algorithm enhances the extraction efficiency for periodic impulsive signals and provides stronger noise suppression. To obtain the optimal parameters $f(n)$, the correlated kurtosis of $x(n)$ is used as the objective function:

$$MCKD_M(T)=\max_{\vec{f}}CK_M(T)=\max_{\vec{f}}\frac{\sum_{n=1}^{N}(\prod_{m=0}^{M}y_{n-mT})^2}{(\sum_{n=1}^{N}y_n^{\,2})^{M+1}} \tag{9}$$

Where, $\vec{f}=(f_1,f_2,\cdots,f_L)^T$.

To determine the optimal filter $f(n)$ that maximizes $CK_M(T)$, the above optimization problem is equivalent to solving the following system of equations:

$$\frac{d}{df_n}CK_M(T)=0,\quad k=1,2,\cdots,L \tag{10}$$

Using matrix representation, the final solution for the filter can be expressed as:

$$\vec{f} = \frac{\| \vec{y} \|^2}{2 \| \vec{A} \|} (X_0 X_0{}^T)^{-1} \sum_{m=0}^{M} X_{mT} B_m \tag{11}$$

2.3 Cross-Correlation Coefficient

The correlation between a frequency band component and the source fault signal directly reflects the degree of fault-related features in the time domain [13]. By decomposing the bearing fault signal, a series of IMF components x_j, can be obtained. The cross-correlation coefficient ρ between each IMF and the original signal x is defined as:

$$\rho(x_j, x) = \frac{\mathrm{cov}(x, x_j)}{\sqrt{D(x_j)}\sqrt{D(x)}} = \left| \frac{\sum_{i=1}^{n} \left(x_j(i) - \overline{x_j} \right) \left(x(i) - \overline{x} \right)}{\sqrt{\sum_{i=1}^{n} \left(x_j(i) - \overline{x_j} \right)^2} \sqrt{\sum_{i=1}^{n} \left(x(i) - \overline{x} \right)^2}} \right| \tag{12}$$

Where, $\overline{x}$ denotes the mean of x;

$\overline{x_j}$ denotes the mean of x_j.

The cross-correlation coefficient quantifies the correlation between each IMF component and the fault signal. A higher cross-correlation coefficient indicates that the IMF component contains more fault-related information, whereas a lower value suggests less relevance to the fault characteristics. When the cross-correlation coefficient of an IMF component is greater than or equal to 0.5, the component is considered an effective component and can be used for signal reconstruction.

2.4 GWO

The GWO is characterized by strong convergence capability and few control parameters, making it effective for parameter optimization tasks. Its unique adaptive convergence factor and feedback mechanism enable a good balance between local exploitation and global exploration, resulting in robust accuracy and fast convergence speed.

In the hunting process, the leading wolf α, along with the subordinate wolves β and δ, guides the search, while the rest of the wolves ω adjust their positions based on α, β, and δ to encircle and hunt the prey. The basic procedure of the GWO algorithm is as follows (Figure 1):

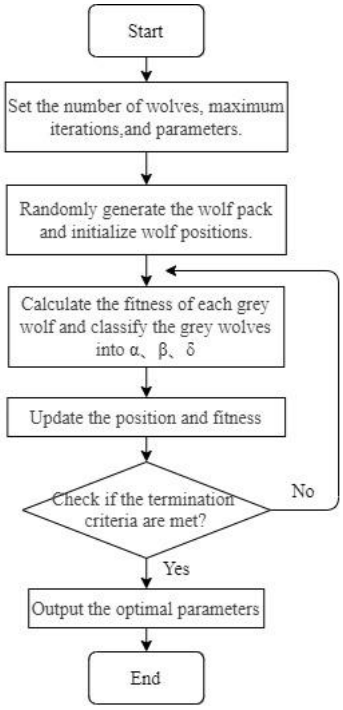

Figure 1 GWO Algorithm Flowchart

2.5 Sample Entropy

Sample entropy measures the complexity of a time series based on the probability of generating new patterns within the

signal. It offers the advantages of requiring no self-matching, fast computation, and high accuracy. The magnitude of the sample entropy is positively correlated with the complexity of the time series: the higher the sequence complexity, the larger the sample entropy; conversely, higher self-similarity (i.e., lower complexity) results in a smaller sample entropy value.

Given a time series $\left\{ X(\mathrm{i}) \middle| 1 \le \mathrm{i} \le N \right\}$, the sample entropy can be calculated as follows:

(1) For a time series of N data points and embedding dimension m, define

$$X(\mathrm{i}) = [\mathrm{x_i}, \mathrm{x_{i+1}}, \mathrm{x_{i+m-1}}] \tag{13}$$

(2) Define the maximum distance between two vectors as:

$$d_{ij} = d[x(i), d(j)] = \max_{k=0,1,\cdots,m-1} \left\{ \left| x(i+k) - x(j+k) \right| \right\} \tag{14}$$

(3) Given a similarity tolerance r, the probability that any two m-length vectors are similar is:

$$B_i^m(r) = \frac{Num(d_{ij} < r)}{N-m}, i = 1, 2, \ldots, N-m+1, i \neq j \tag{15}$$

(4) Compute the mean of B_i^m (r):

$$B^m(r) = \frac{1}{N-m+1} \sum_{i=1}^{N-m+1} B_i^m(r) \tag{16}$$

(5) Increase the embedding dimension to m+1 and repeat steps (13)~(16) to obtain B_i^m (r+1) for B^m (r+1);
(6) The sample entropy is finally defined as:

$$SamEn(m, r) = \lim_{N \to \infty} \left[-\mathrm{In}\left(\frac{B^{m+1}(r)}{B^m(r)} \right) \right] \tag{17}$$

(7) When N is finite, the sample entropy can be expressed as:

$$SamEn(m, r) = -\mathrm{In}\left(\frac{B^{m+1}(r)}{B^m(r)} \right) \tag{18}$$

In summary, the values of m and r significantly influence the computed sample entropy. Different choices of embedding dimension m and similarity tolerance r will yield different sample entropy results for the same time series.

2.6 VMD-GWO-MCKD Method

Based on the strong decomposition capability of the VMD algorithm for non-stationary vibration signals, the excellent noise reduction performance of the MCKD algorithm, and the efficient parameter optimization capability of the GWO algorithm, this section proposes a VMD-GWO-MCKD method for diagnosing wheel OOR faults. The detailed procedure is as follows:
Step 1: Decompose the fault signal using VMD to obtain multiple IMF components.
Step 2: Calculate the cross-correlation coefficients between each IMF component and the original signal, and select the IMF components that meet the combined criteria for signal reconstruction.
Step 3: Use the Grey Wolf Optimization (GWO) algorithm to search for the optimal MCKD parameters by employing the minimum sample entropy principle, obtaining the optimal parameters L_m and T_m;
Step 4: Input the optimal parameters L_m and T_m into the MCKD for denoising processing.
Step 5: Perform Hilbert envelope spectrum analysis on the denoised signal to identify the fault type.

3 VIBRATION TEST AND ANALYSIS

3.1 Test Scheme

In this experiment, a three-channel vibration sensor with a measurement range of 50 g and a bandwidth of 5000 Hz was employed to capture the longitudinal, lateral, and vertical vibration signals. The sensors were installed at three positions: the end of the bogie frame, the bogie frame near the air spring, and the axle box. Straight track tests were conducted under the AW0 working condition for both worn wheels and re-profiled wheels to evaluate the wheel polygonal wear condition and radial runout (Figure 2).

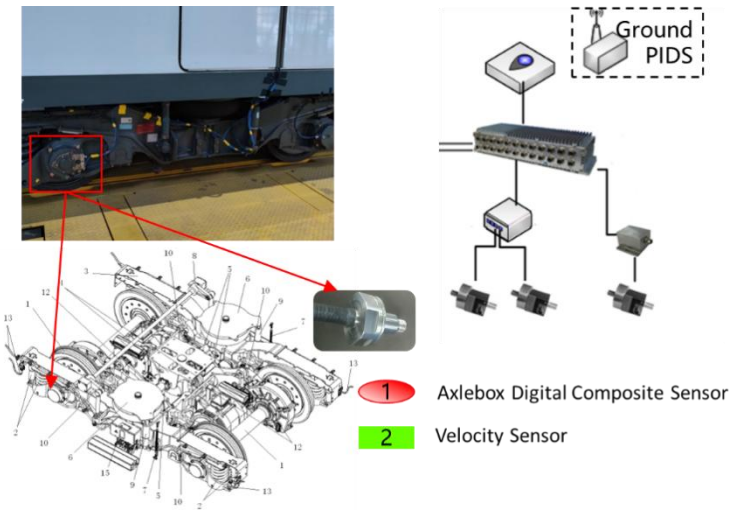

Figure 2 Rotating Machinery Failure Simulation Fundamentals Test Bench

3.2 VMD-GWO-MCKD Analysis

The time-domain waveform of the wheel OOR fault signal is presented in Figure 3.

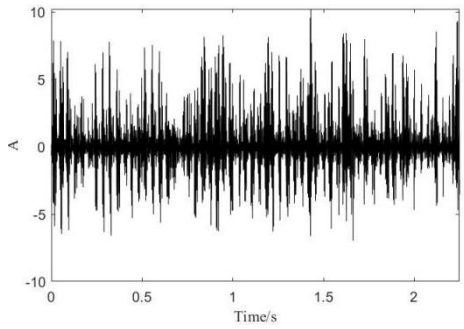

Figure 3 Time-domain Waveform of the Fault Signal

Using the center frequency observation method, the number of decomposition modes for VMD was set to K=7. The decomposition results are displayed in Figure 4. After obtaining the IMF components, their corresponding cross-correlation coefficients with the original signal were calculated, as summarized in Table 1. IMF components with cross-correlation coefficients greater than 0.3 were selected for signal reconstruction.

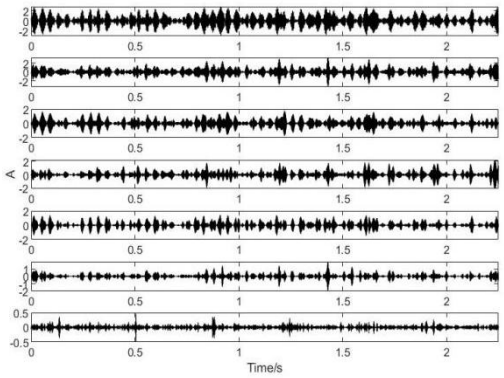

Figure 4 VMD Analysis Results

Table 1 Cross-correlation Coefficients of Each IMF Component

IMF	IMF_1	IMF_2	IMF_3	IMF_4
Cross-correlation coefficient	0.6612	0.5447	0.3777	0.364

IMF	IMF_5	IMF_6	IMF_7
Cross-correlation coefficient	0.2997	0.2608	0.0747

The GWO-MCKD algorithm was then applied, with the number of grey wolves set to 20 and the maximum number of iterations set to 20. The optimal parameters were determined based on the minimum sample entropy principle. The search range for the MCKD filter length L was [50, 500], and for the deconvolution period T was [100, 500]. The convergence curve is illustrated in Figure 5.

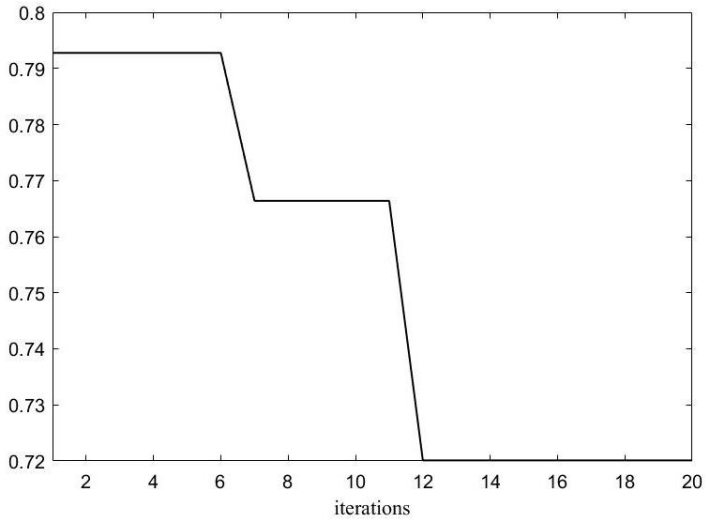

Figure 5 Convergence Curve

As the number of iterations increases, the sample entropy gradually stabilizes, indicating that the population has converged to a near-global optimal solution. The computation time of the GWO optimization algorithm was 852 seconds, yielding optimal parameters of $L_m = 300$ and $T_m = 524$. By inputting the optimal combination [Lm, Tm] into the MCKD algorithm, the resulting filtered signal is shown in Figure 6.

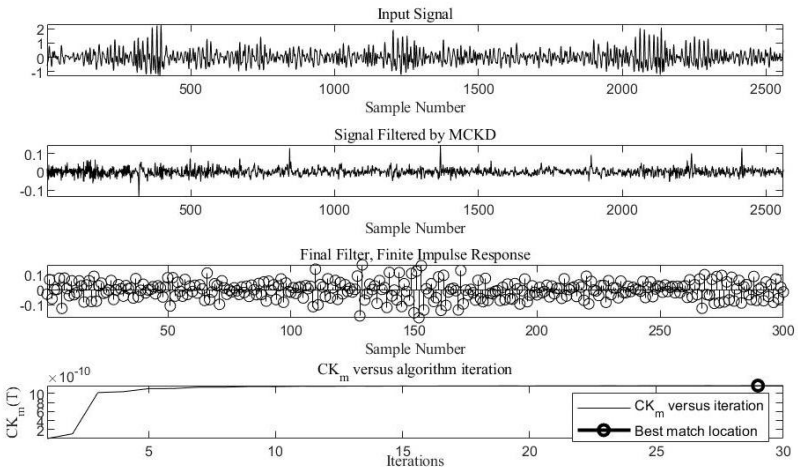

Figure 6 MCKD Decomposition

The envelope spectrum obtained using the VMD-GWO-MCKD method is shown in Figure 7.

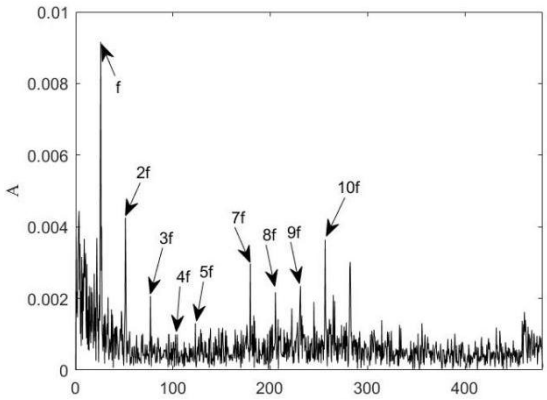

Figure 7 Hilbert Envelope Spectrum

As illustrated in Figure 6, the VMD-GWO-MCKD envelope spectrum clearly reveals the fault-induced impact features embedded in the dynamic signal, with significant suppression of noise and other interference components. The fundamental fault frequency f and its harmonic multiples are distinctly highlighted, with a notable amplitude enhancement observed at the 10th harmonic. This confirms the presence of a decagonal (10-lobed) wheel OOR fault, which aligns with the actual measured condition. These results demonstrate that the proposed VMD-GWO-MCKD algorithm effectively extracts the characteristic features of the wheel OOR fault, validating the method's feasibility and robustness.

The envelope spectrum of the vibration signal after wheel re-turning (reprofiling) is shown in Figure 8.

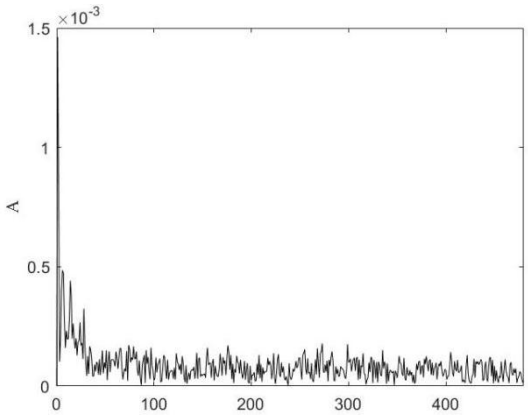

Figure 8 Hilbert Envelope Spectrum after Wheel Re-turning

As shown in Figure 8, no harmonic frequency components with integer multiples are detected after the wheel reprofiling, and the maximum amplitude is in the order of 10^{-3}. This indicates the absence of evident periodic fault-related vibration features, which is consistent with the actual condition of the reprofiled wheel.

4 CONCLUSION

When a train wheel develops OOR defects, significant vibrations and impact impulses occur during wheel-rail interactions, potentially affecting operational safety and ride comfort. To address this issue, this study proposed a fault feature extraction method for wheel OOR based on VMD and GWO for optimal parameter tuning of MCKD. Experimental validation using measured vibration data demonstrates that the VMD-GWO-MCKD method can accurately identify wheel OOR faults. By analyzing the extracted fundamental frequency and its harmonics, the method enables precise detection and characterization of polygonal wheel defects.

COMPETING INTERESTS

The authors have no relevant financial or non-financial interests to disclose.

REFERENCES

[1] Chen X, Li J H, Liu W S, et al. Research on countermeasures for wheel out-of-roundness of domestic Type A metro vehicles. Locomotive & Rolling Stock Technology, 2025, 61(1): 50-54.

[2] Hou S J. Initial Research on the Automatic Computer Inspection System on Wheel Treads. Railway Vehicles, 2001, 39(12): 3.

[3] Ji J C. Research on online dynamic measurement method of wheelset geometric parameters: Beijing Jiaotong University. 2015.
[4] Zhang J J, Ma Z Q, Wang M Q, et al. Rolling bearing fault feature extraction based on VMD and autocorrelation analysis. Journal of Electronic Measurement and Instrumentation, 2017, 31(9): 7.
[5] Sun K, Zhang L, Wang F Z. Partial discharge signal denoising method based on variational mode decomposition and singular value decomposition. Journal of Henan Polytechnic University (Natural Science), 2020, 39(6): 8.
[6] Fei H B, Zhang C, Wu L, et al. Denoising and impact feature enhancement method for weak fault signals based on VMD-MCKD. Mechanical & Electrical Engineering, 2025, 42(2): 237-246.
[7] Tang J, Zhao Q. Motor rolling bearing fault diagnosis based on MVMD energy entropy and GWO-SVM. Journal of Vibroengineering, 2023, 25(6): 1096-1107.
[8] Saari J, Strömbergsson D, Lundberg J, et al. Detection and identification of windmill bearing faults using a one-class support vector machine (SVM). measurement, 2019, 137: 287-301.
[9] Dragomiretskiy K, Zosso D. Variational mode decomposition. IEEE transactions on signal processing, 2013, 62(3): 531-544.
[10] Wang X, You C, Li X, et al. Chatter feature extraction for milling thin-walled parts based on GWO-VMD and CMSE. The International Journal of Advanced Manufacturing Technology, 2025, 1-14.
[11] Yang J, Liu W, Li S, et al. editors. Fault Diagnosis Method of Bearings Based on RandWPSO-VMD-MCKD. Journal of Physics Conference Series, 2025, 2999(1): 012052. DOI: 10.1088/1742-6596/2999/1/012052.
[12] Zhao L, Chi X, Li P, et al. Incipient fault feature enhancement of rolling bearings based on CEEMDAN and MCKD. Applied Sciences, 2023, 13(9): 5688.
[13] Stylianou O, Susi G, Hoffmann M, et al. Multiscale detrended cross-correlation coefficient: estimating coupling in non-stationary neurophysiological signals. Frontiers in Neuroscience, 2024, 18: 1422085.